Van Der Waals Revisited

Klaus Bärwinkel [a],*

[a]*Universität Osnabrück, Fachbereich Physik, D-49069 Osnabrück, Germany*

Jürgen Schnack [b]

[b]*Universität Bielefeld, Fakultät für Physik, Postfach 100131, D-33501 Bielefeld, Germany*

Abstract

The van-der-Waals version of the second virial coefficient is not far from being exact if the model parameters are appropriately chosen. It is shown how the van-der-Waals resemblance originates from the interplay of thermal averaging and superposition of scattering phase shift contributions. The derivation of the two parameters from the quantum virial coefficient reveals a fermion-boson symmetry in non-ideal quantum gases. Numerical details are worked out for the Helium quantum gases.

1 Occupation number statistics and the van-der-Waals model

Occupation number statistics for $N = n\Omega$ non-interacting distinguishable quantum particles in a volume Ω yields the entropy density functional

$$s = \frac{k_B}{\Omega} \int \mathrm{d}^3 p \, \rho(\vec{p}) \, \nu_{\vec{p}} (1 - \ln \nu_{\vec{p}}) \tag{1}$$

where $\nu_{\vec{p}}$ is the average occupation number of a single-particle energy eigenstate. (In order to be more general, one may consider indistinguishable quasi-particles, see e.g. [1]). These eigenstates are enumerated by corresponding

---

* Tel: ++49 541 969-2694; fax: -2670; Email: klaus.baerwinkel@uni-osnabrueck.de
**Tel: ++49 521 106-6193; fax -6455; Email: jschnack@uni-bielefeld.de

points $\vec{p}$ in momentum space, the density of which is $\rho(\vec{p})$. k_B denotes Boltzmann's constant.

A hard-core like repulsive interaction is taken into account by the van-der-Waals ansatz

$$\rho(\vec{p}) = (\Omega - Nb)/(2\pi\hbar)^3 \; . \tag{2}$$

Here the "single-particle volume" b is our first van-der-Waals parameter. We consider elementary cells of volume

$$v_{e\ell} = \frac{\Omega}{\rho(\vec{p})} = \frac{(2\pi\hbar)^3}{1 - nb} \tag{3}$$

in six-dimensional phase space (μ-space) and the one-particle distribution function

$$f(\vec{p}) = \nu_{\vec{p}}/v_{e\ell} \; . \tag{4}$$

The entropy density

$$s = k_B \int \mathrm{d}^3p \, f(\vec{p}) \, (1 - \ln(f(\vec{p})v_{e\ell})) \tag{5}$$

is then to be maximized as a functional of f subject to the constraints of fixed particle density

$$n = \int \mathrm{d}^3p \, f(\vec{p}) \tag{6}$$

and fixed energy density

$$u = \int \mathrm{d}^3p \, f(\vec{p}) \, \epsilon_{\vec{p}} \; . \tag{7}$$

According to the second van-der-Waals ansatz, each particle has its classical kinetic energy and is in the potential field of interaction with the other particles, i.e.

$$\epsilon_{\vec{p}} = \frac{p^2}{2m} - an \; , \tag{8}$$

where a is the second van-der-Waals parameter. Clearly, the treatment of correlations is incomplete in this model.

The energy density now becomes

$$u = \int \mathrm{d}^3p \, \frac{p^2}{2m} f(\vec{p}) - an^2 \; . \tag{9}$$

From the principle of maximum entropy s and using the temperature definition

$$T = [(\partial s/\partial u)_n]^{-1} \tag{10}$$

one finds f to be the Maxwellian

$$f(\vec{p}) = n(2\pi m k_B T)^{3/2} \exp\left\{ -\frac{p^2}{2m k_B T} \right\} \; . \tag{11}$$

This leads to

$$s = nk_B \left(\frac{5}{2} - \ln \left(\frac{n\lambda^3}{1 - nb} \right) \right) \tag{12}$$

with the thermal wavelength

$$\lambda = (2\pi\hbar)/\sqrt{2\pi m k_B T} \tag{13}$$

and to

$$u = \frac{3}{2}nk_B T - an^2 . \tag{14}$$

Then the pressure formula

$$P_{eq} = -\frac{1}{n^2} \left(\frac{\partial u}{\partial n} \right)_s \tag{15}$$

results in the van-der-Waals equation of state:

$$P_{eq} = \frac{nk_B T}{1 - nb} - an^2 . \tag{16}$$

Because of the insufficient treatment of two-particle correlations, this formula will allow a quantitatively satisfying fit for real systems only if $n\lambda^3$ is sufficiently small. Consequently, the van-der-Waals version of the second virial coefficient $B(T)$ is a good approximation if the temperature is not too low:

$$B(T) \approx b - \frac{a}{k_B T} . \tag{17}$$

The appropriate choice of the parameters a and b is dealt with in the following sections.

2   Heuristics of the van-der-Waals parameters

The van-der-Waals model can be introduced via corresponding approximations to the radial distribution function. To this end consider first the average potential energy of $N = n\Omega$ mutually interacting classical particles:

$$W_{pot} = \frac{1}{2} < \sum_{i \neq j} V(|\vec{r}_i - \vec{r}_j| > . \tag{18}$$

With the radial distribution function defined by

$$g(|\vec{r}\,' - \vec{r}\,''| >= n^{-2} < \sum_{i \neq j} \delta(\vec{r}\,' - \vec{r}_i)\delta(\vec{r}\,'' - \vec{r}_j) > \tag{19}$$

one gets

$$W_{pot} = N\frac{n}{2} \int \mathrm{d}^3 r \, g(r) \, V(r) . \tag{20}$$

Now $g(r)$ has its density expansion

$$g(r) = g_0(r) + ng_1(r) + n^2 g_2(r) + \dots \ . \tag{21}$$

The energy of a single classical particle is therefore – apart from higher-order density contributions – given by eq. (8) with

$$a = -\frac{1}{2} \int d^3r \, V(r) \, g_0(r) \ . \tag{22}$$

In view of the classical limit

$$g_{0,cl}(r) = \exp\left\{-\frac{V(r)}{k_B T}\right\} \tag{23}$$

with a Lennard-Jones potential (see below, eq. (35)), there will be a cut-off radius r_* such that the approximation

$$g_0(r) = \begin{cases} 0 \ , & \text{for } r < r_* \\ 1 \ , & \text{for } r > r_* \end{cases} \tag{24}$$

with a constant r_* is applicable in a considerable range of temperature. This eventually fixes the parameter a as

$$a = -\frac{1}{2} \int_{r \geq r_*} d^3r \, V(r) \ . \tag{25}$$

On the other hand, both the parameters a and b may be introduced by first expressing the second virial coefficient in terms of g_0 [2],

$$B(T) = \frac{1}{2} \int d^3r \, (1 - g_0(r)) \tag{26}$$

and employing the closer approximation

$$g_0(r) = \begin{cases} 0 & , \quad \text{for } r < r_* \\ 1 - \frac{V(r)}{k_B T} & , \quad \text{for } r > r_* \end{cases} \ . \tag{27}$$

Comparison with the van-der-Waals version of $B(T)$ (eq. (17)) then yields a as given by eq. (25) and

$$b = \frac{2\pi}{3} r_*^3 \ . \tag{28}$$

The closer approximation of g_0 – if inserted in eq. (22) – would cause a slight dependence of a on temperature. This must be negligible for the van-der-Waals model to be acceptable.

In the next section, formulae (17), (25), and (28) will be substantiated by numerical analysis of the exact quantum mechanical virial coefficient, and the cut-off radius r_* will be determined.

4

3 The exact virial coefficient and its van-der-Waals limit

3.1 Substantiation of the model

The exact theory [3] for boson or fermion gases with their two-particle interaction having, possibly, bound state energies E_i gives the second virial coefficient as a sum of four terms:

$$B(T) = \mp 2^{-5/2}\lambda^3 - 2^{3/2}\lambda^3 \sum_i e^{-E_i/k_BT} + \ll G_\pm \gg + \frac{\ll F_\pm \gg}{k_BT} \qquad (29)$$

with the quantities $\ll G_\pm \gg$ and $\ll F_\pm \gg$ being explained below (eqs. (37), (38)) and with the upper (lower) sign valid for bosons (fermions). Evidently, formula (17) is justified if $\ll F_\pm \gg$ and $\ll G_\pm \gg$ prove to be practically constant in a relevant range of temperature where the other contributions are negligible. The double bracket is our notation for the thermal average of momentum dependent functions, e.g.

$$\ll F \gg = \int_0^\infty \mathrm{d}p\, w(p)\, F(p) \;, \qquad (30)$$

with the thermal weight function

$$w(p) = 4\pi \, (\pi m k_B T)^{-3/2} \, p^2 \exp\left\{ -\frac{p^2}{m k_B T} \right\} \;. \qquad (31)$$

The functions $F_\pm$ and $G_\pm$ may be expressed in terms of the properly (anti-) symmetrized momentum representation of the two-particle operator

$$\mathcal{T}(z) = V - V\frac{1}{H-z}V \;,\; \mathcal{T}'(z) = \frac{d}{dz}\mathcal{T}(z) \;, \qquad (32)$$

with $H = H_{kin} + V$ being the Hamiltonian of relative motion:

$$F_\pm(p) = -\frac{1}{2}(2\pi\hbar)^3 \Re\left(< \vec{p}\,|\mathcal{T}_\pm(E_p + i\epsilon > |\vec{p}>\right) \;,\; E_p = \frac{p^2}{m} \;, \qquad (33)$$

$$G_\pm(p) = \frac{\pi}{2}(2\pi\hbar)^3 \int \mathrm{d}^3q\, \delta(E_p - E_q) \cdot \qquad (34)$$
$$\cdot \Im\left(< \vec{p}\,|\mathcal{T}_\pm(E_q + i\epsilon)|\vec{q}><\vec{q}\,|\mathcal{T}'_\pm(E_q + i\epsilon)|\vec{p}>\right) \;.$$

Our graphics Fig. 1 for $F_\pm$ and $G_\pm$ rely on the numerical evaluation for bosons (^{4}He atoms) interacting via a Lennard-Jones potential lacking bound states [4] and fermions (same mass and same interaction as ^{4}He):

$$V(r) = 4V_0\left[\left(\frac{\sigma}{r}\right)^{12} - \left(\frac{\sigma}{r}\right)^6\right] \;;\; V_0/k_B = 10.22\mathrm{K}, \sigma = 2.56\mathrm{\AA} \;. \qquad (35)$$

5

The (anti-) symmetrized $\mathcal{T}$-matrix is – up to a multiplicative constant – nothing else but the scattering amplitude

$$f_\pm(p, \theta) = -\pi^2 m \hbar < \vec{p} \, |\mathcal{T}_\pm(E_p + i\epsilon)|\vec{q} > \, , \; |\vec{p}| = |\vec{q}| \, , \; \vec{p} \cdot \vec{q} = p^2 \cos \theta \, . \quad (36)$$

An alternative representation for $F_\pm$ and $G_\pm$ can therefore be given in terms of scattering phase shifts δ_ℓ which complies with the Beth-Uhlenbeck result for $B(T)$ [5,6]:

$$F_\pm = \frac{4\pi\hbar^2}{m} f_\pm(p, 0) = \frac{4\pi\hbar^2}{m} \frac{\hbar}{2p} \sum_\ell {}^\pm (2\ell + 1) \sin 2\delta_\ell(p) \quad (37)$$

$$G_\pm(p) = -4\pi\hbar \frac{\hbar^2}{p^2} \sum_\ell {}^\pm (2\ell + 1) \sin^2[\delta_\ell(p)] \frac{\partial \delta_\ell(p)}{\partial p} \, . \quad (38)$$

The summation runs over even ℓ for bosons and odd ℓ for fermions.
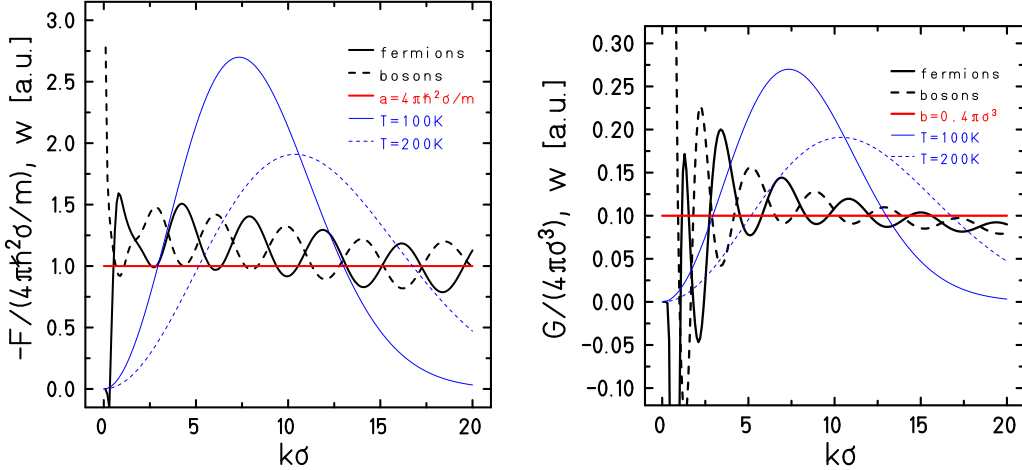

Fig. 1. Functions $F_\pm$ and $G_\pm$ for bosons (^{4}He atoms) interacting via the Lennard-Jones potential (35) and fermions with the same mass and same interaction. The thermal weight function is given for two temperatures. The horizontal line on the l.h.s. marks the value of a as given by (59) and on the r.h.s. the value of b as given by (58).

A remark on the units and dependencies of $F_\pm$, $G_\pm$ will be fitting here. Let $p = \hbar k$ and choose $\tilde{r} = r/\sigma$ as the dimensionless radial coordinate. Then the dimensionless version of the radial wave equation with eigenvalue E_p becomes

$$u_\ell''(\tilde{r}) + \left\{ \text{Re} \; (\tilde{r}^{-12} - \tilde{r}^{-6}) + \ell(\ell + 1)\tilde{r}^{-2} \right\} u(\tilde{r}) = (k\sigma)^2 u_\ell(\tilde{r}) \quad (39)$$

where

$$\text{Re} = \frac{4V_0 m \sigma^2}{\hbar^2} \quad (40)$$

is the "Reynolds number". Given the appropriate behavior of u_ℓ for $\tilde{r} \to 0$,

the asymptotic behavior for $\tilde{r} \to \infty$ exhibits the phase shift δ_ℓ:

$$u_\ell(\tilde{r}) \longrightarrow \sin(k\sigma\tilde{r} - \frac{\ell}{2}\pi + \delta_\ell) \ . \tag{41}$$

Thus the only dependency of δ_ℓ is on Re and $k\sigma$. Consequently, with some functions $\varphi = \varphi(\mathrm{Re}, k\sigma)$ and $\gamma = \gamma(\mathrm{Re}, k\sigma)$

$$F_\pm = \frac{4\pi\hbar^2\sigma}{m} \cdot \varphi(\mathrm{Re}, k\sigma) = 16\pi V_0 \ \sigma^3 \ \frac{\varphi(\mathrm{Re}, k\sigma)}{\mathrm{Re}} \ , \tag{42}$$

$$G_\pm = 4\pi\sigma^3 \ \gamma(\mathrm{Re}, k\sigma) \ . \tag{43}$$

In each of our graphics the boson and the fermion function refer to the same value of Re. With the potential data of eq. (35) and with m the mass of ^{4}He we obtain Re ≈ 22.1.

The weight function $w = w(p)$ (eq. (31)) assumes its maximum at $p_{\max} = \hbar k_{\max}$ with

$$k_{\max}\sigma = \left(\frac{100\mathrm{Re}}{4 \cdot 10, 22}\right)^{1/2} \cdot \left(\frac{T}{100K}\right)^{1/2} \tag{44}$$

and it is easily seen that above $T = 100K$ the weight functions samples rather large values of $k\sigma$ ($k\sigma \gtrsim 10$). For high values of $k\sigma$ Fig. 1 shows that both F_+ and F_- oscillate about a common approximately constant value. This reflects the nearly hard-core likeness of the repulsive part of the Lennard-Jones potential. Let us therefore consider, for comparison, a pure hard-core repulsion with radius σ.

In this special case

$$\tan\delta_\ell = j_\ell(k\sigma)/y_\ell(k\sigma) \tag{45}$$

holds, with j_ℓ and y_ℓ denoting the spherical Bessel functions

$$j_\ell(z) = z^n \left(-\frac{1}{z}\frac{d}{dz}\right)^n \frac{\sin z}{z} \ , \ y_\ell(z) = z^n \left(\frac{d}{dz}\right)^n \frac{\cos z}{z} \ . \tag{46}$$

Invoking

$$\sin 2\delta_\ell = 2\frac{\tan\delta_\ell}{1 + \tan^2\delta_\ell} \tag{47}$$

and the asymptotic behavior

$$\lim_{z\to\infty} \left(j_\ell^2(z) + y_\ell^2(z)\right) = 1/z^2 \ , \tag{48}$$

one arrives at

$$(F_+^{hc} - F_-^{hc})_{asy} = \frac{4\pi\hbar^2\sigma^2 k}{m} \sum_{\ell=0}^{\infty}(-1)^{\ell+1}(2\ell+1) \ j_\ell(k\sigma) \ y_\ell(k\sigma) \ . \tag{49}$$

Now – as a marginal case of formula 10.1.46 in [7] –

$$\sum_{\ell=0}^{\infty}(-1)^{\ell+1}\,(2\ell+1)\,j_\ell(z)\,y_\ell(z) = \frac{\cos 2z}{2\sigma} \tag{50}$$

and consequently

$$(F_-^{hc} - F_+^{hc})_{asy} = \frac{2\pi\hbar^2\sigma}{m}\cos(2k\sigma)\;. \tag{51}$$

This is the asymptotic ($k\sigma \to \infty$) result for the hard-core system. It is compared with ($F_- - F_+$) for the Lennard-Jones system in Fig. 2. The behavior is very similar both in terms of amplitude and frequency. A slight decrease of σ with increasing k in formula (51) would still improve the agreement. This reflects the fact that the Lennard-Jones potential appears the softer the higher the particles' energy is.
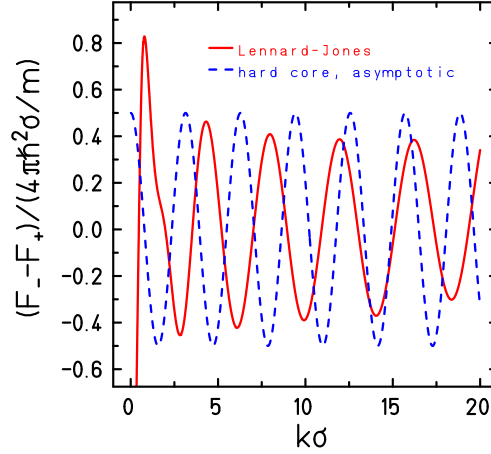

Fig. 2. Comparison of ($F_- - F_+$) for the Lennard-Jones system (solid curve) with the asymptotic result for the hard core system (dashed curve).

As for $G_\pm$, an oscillation about a common constant value is once again seen, compare the r.h.s. of Fig. 1. In contrast to the case of $F_\pm$, however, the oscillatory amplitude of the difference is clearly decreasing. Not surprisingly, this feature can again be derived analytically for a pure hard-core repulsion with radius σ.

To this end, $G_\pm$ (eq. (38)) is first rewritten as

$$G_\pm = \frac{2\pi\sigma^3}{(k\sigma)^2}\frac{\partial}{\partial(k\sigma)}\sum_\ell {}^\pm(2\ell+1)\left(\frac{1}{2}\sin 2\delta_\ell(k\sigma) - \delta_\ell(k\sigma)\right) \tag{52}$$

and then employed for the hard-core system. With the aid of eqs. (45), (47), and (48) the asymptotic ($k\sigma \to \infty$) tail of ($G_+^{hc} - G_-^{hc}$) is found to be

$$(G_+^{hc} - G_-^{hc})_{asy} = 2\pi\sigma^3\sum_{\ell=0}^{\infty}(-1)^\ell\,(2\ell+1)\,j_\ell(k\sigma)\,y_\ell'(k\sigma)\;. \tag{53}$$

8

After replacing (for $k\sigma \to \infty$) y'_ℓ by j_ℓ, one can apply formula 10.1.51 in [7],

$$\sum_{\ell=0}^{\infty} (-1)^\ell (2\ell+1) j_\ell^2(z) = \frac{\sin 2z}{2z} \ ,\tag{54}$$

and hence

$$(G_+^{hc} - G_-^{hc})_{asy} = 2\pi\sigma^3 \frac{\sin 2k\sigma}{2k\sigma} \ .\tag{55}$$

The difference $(G_+ - G_-)$ for the Lennard-Jones system is compared with this result in Fig. 3. Again, the behavior is very similar both in terms of amplitude and frequency, also the phase difference increases only slightly.
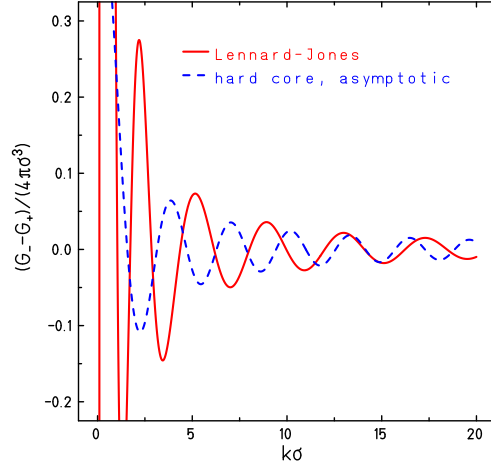

Fig. 3. Comparison of $(G_- - G_+)$ for the Lennard-Jones system (solid curve) with the asymptotic result for the hard core system (dashed curve).

3.2   The cut-off radius

Instead of eq. (27) a continuous ansatz for $g_0(r)$ may be used:

$$g_0(r) = \begin{cases} 0 & , \ \text{for } r \leq_* \\ 1 - \exp\left(-\alpha \frac{r-r_*}{r_*}\right) + \frac{V(r) - V(r_*)\exp(-\alpha\frac{r-r_*}{r_*})}{k_B T} & , \ \text{for } r \geq r_* \end{cases}\tag{56}$$

with the potential $V(r)$ according to eq. (35). Equation (27) is reproduced for $\alpha \to \infty$. The values of r_*/σ and α follow from the van-der-Waals condition

$$b - \frac{a}{k_B T} = \frac{1}{2} \int d^3 r (1 - g_0(r))\tag{57}$$

where

$$b = 0.4\pi\sigma^3\tag{58}$$

and

$$a = \frac{4\pi\hbar^2\sigma}{m} = \frac{16\pi}{\text{Re}} \cdot V_0\sigma^3\tag{59}$$

9

is estimated in view of Fig. 1 (horizontal lines). Then

$$r_* = x^{-1/3}\sigma \tag{60}$$

where x is the solution of

$$x = \frac{3}{\mathrm{Re}} + 0.3x^2 + \frac{2}{3}x^3 - 0.3x^4 \tag{61}$$

with $0.2x > 1/3$. The parameter α follows from

$$0.2x - 1/3 = \frac{1}{\alpha} + \frac{2}{\alpha^2} + \frac{2}{\alpha^3} \ . \tag{62}$$

Then a has the following representation in terms of the Reynolds number Re and the Lennard-Jones parameters V_0 and σ:

$$a = \frac{4\pi V_0 \sigma^3}{3}\left(x - \frac{1}{3}x^3\right) \ , \tag{63}$$

where $x = x(\mathrm{Re})$ is the solution of eq. (61), which allows a positive α in eq. (62). For Re= 22.1 we obtain $x = 1.88$ and $\alpha = 25.6$. Therefore, in our ansatz (56) $g_0(r)$ is close to its limit for $\alpha \to \infty$, which is given in eq. (27).

Summary

The summary of our elaboration is that for a large region of temperature the functions $\ll F_\pm \gg = a$ and $\ll G_\pm \gg = b$ may be nearly considered as constants, i.e. not depending on temperature, see Fig. 1. Moreover, the respective kind of statistics (Bose-Einstein or Fermi-Dirac) does not matter. This constitutes a fermion-boson symmetry in non-ideal quantum gases. For ideal quantum gases such symmetries are known for about ten years [8,9].

Acknowledgment

References

[1] K. Bärwinkel, J. Schnack, U. Thelker, Quasi-particle picture for monatomic gases, Physica A 262 (1999) 496.

[2] K. Bärwinkel, S. Großmann, Pair distribution function of moderately dense quantum fluids, Z. Phys. 230 (1970) 141.

[3] B. Baumgartl, Second and third virial coefficient of a quantum gas from 2-particle scattering amplitude, Z. Phys. 198 (1967) 148.

[4] J. E. Kilpatrick, M. F. Kilpatrick, Discrete energy levels associated with the Lennard-Jones potential, J. Chem. Phys. 19 (1951) 930.

[5] G. Uhlenbeck, E. Beth, The quantum theory of the non-ideal gas. I. deviations from the classical theory, Physica 3 (1936) 729.

[6] G. Uhlenbeck, E. Beth, The quantum theory of the non-ideal gas. II. behaviour at low temperatures, Physica 4 (1937) 915.

[7] M. Abramovitz, I. Stegun (Eds.), Handbook of Mathematical Functions, Dover, New York, 1973.

[8] M. H. Lee, Equivalence of ideal gases in two dimensions and Landen's relations, Phys. Rev. E 55 (1997) 1518.

[9] H.-J. Schmidt, J. Schnack, Thermodynamic fermion-boson symmetry in harmonic oscillator potentials, Physica A 265 (1999) 584.